Lithuanian Journal of Physics, Vol. **61**, No. 3, pp. 161–168 (2021)

DEPOSITION OF COLLOIDAL METAL NANOPARTICLES ON ZINC OXIDE NANORODS AND THEIR INFLUENCE ON VISIBLE PHOTOLUMINESCENCE

D. Kulmatova [a, b], M. Baitimirova [a], U. Malinovskis [a], C.-F. Chang [c], Y. Gu [d], A. Tamulevičienė [e], D. Erts [a, f], and J. Prikulis [a]

[a] *Institute of Chemical Physics, University of Latvia, 19 Raina Blvd., 1586 Riga, Latvia*
[b] *National University of Uzbekistan, Vuzgorodok, 100174 Tashkent, Uzbekistan*
[c] *Department of Environmental Science and Engineering, Tunghai University, 40704 Taichung, Taiwan*
[d] *Department of Chemical and Materials Engineering, Tunghai University, 40704 Taichung, Taiwan*
[e] *Institute of Materials Science, Kaunas University of Technology, K. Baršausko 59, 51423 Kaunas, Lithuania*
[f] *Department of Chemistry, University of Latvia, 19 Raina Blvd., 1586 Riga, Latvia*
Email: juris.prikulis@lu.lv

Received 18 December 2020; revised 12 April 2021; accepted 15 April 2021

We examine the influence of colloidal Au and Ag nanoparticles (NP) on hydrothermally grown ZnO nanorods (NR). Individual 60 nm diameter NP and small NP assemblies without formation of large aggregates were deposited on poly-L-lysine covered NR films using the dip-coating method. The evaluation of morphological and optical properties of the obtained ZnO-metal hybrids was done using scanning electron microscopy, photoluminescence (PL) and diffuse reflection spectroscopy. The presence of Au NP selectively suppressed the PL components near 560 nm wavelength associated with ZnO surface defects, whereas equally sized Ag NP resulted in a much smaller change of PL signal, barely above the noise level. The presented results may be useful for tuning the optical properties of hybrid materials in development of sensor or photovoltaic devices.

Keywords: ZnO nanostructures, plasmonic metal nanoparticles, templated deposition, dip coating

PACS: 73.20.Mf, 82.70.Dd, 78.55.-m

1. Introduction

An increasing demand exists for cost-effective nanostructured substrates for the design of colorimetric sensors in the visible detection range [1]. Hybrid substrates that combine nanostructures of different materials have a great potential for development of sensor applications. For instance, substrates containing metal oxide nanostructures and noble metal nanoparticles (NP) have been demonstrated in development of new biosensors [2–6]. In ZnO hybrid systems with noble metals, localized surface plasmon resonances (LSPR) in metal NP can be used for enhancement and quenching of ZnO photoluminescence (PL) [2]. Further application examples of ZnO nanorods (NR) decorated with plasmonic NP include photovoltaic energy conversion [7], local heating and photocatalytic reactions [8].

ZnO is one of the most studied metal oxide semiconductor materials due to its accessibility and combination of unique features, including a wide bandgap, large exciton-binding energy, piezoelectric properties and stability at room temperature (RT) [9]. PL spectra of bulk and nanostructured ZnO are rich with components that correspond to different physical processes, which coexist in the ZnO structure, including excitonic recombination [10], transitions between levels associated with impurities, oxygen and zinc vacancies, antisites, interstitial and surface defects [11–13]. The latter

become especially important in nanostructured forms of ZnO due to the increased surface to volume ratio. For example, it was shown that the relative intensity of defect PL in comparison to excitonic PL is larger for ZnO NR with smaller diameters [14]. The PL signal from the surface defects is of obvious interest for sensor applications since the surface can directly interact with the analyte in the gas and liquid phase [15]. Furthermore, defect PL can be excited and detected in the visible range at RT [16] eliminating the need of sophisticated ultraviolet optics and cryogenics, which is important in practical implementation of sensor devices.

Various synthesis techniques have been developed for fabrication of ZnO nanostructures, including chemical bath deposition [17], hydrothermal growth [18], chemical gas reactions [19], atomic layer deposition [20] and others [21]. Deposition of metals on ZnO NR can be achieved by different methods, such as sputtering [4], photochemical reactions [8, 22], or electrodeposition [6]. A common difficulty with the above *bottom-up* techniques is to produce NP with a well-defined size and shape, which are the key parameters that determine the LSPR properties [23]. Lithographic *top-down* fabrication of hybrid systems with the predetermined geometry for plasmonic PL enhancement is possible [24], but it is a relatively time consuming and expensive process for scalable production. Masked deposition through self-organized templates such as nanoporous anodic alumina (NAA) films [25] can produce exceptionally high density arrays of isolated NP, that support new collective resonant modes [26] for interferometric sensors, however, particle properties in this technique cannot be tuned independently from template geometry.

Highly monodisperse metal NP can be synthesized in a colloidal form [27]. However, during deposition of colloids on surfaces particles typically form large aggregates [28], therefore extra measures must be taken to control the cluster formation with desired optical properties [29].

In this work, we placed individual Au and Ag NP and small assemblies from colloidal solutions on hydrothermally grown ZnO NR using capillary force assisted (CFA) deposition that was recently developed for an isolated NP array assembly on the NAA surface [30]. The ZnO surface coating with poly-L-lysine (PLL) prior to NP deposition significantly increased the number of NP per unit area without aggregation [31] and enabled the optical detection of material dependent LSPR and PL signal.

2. Experiment

Zinc acetate dihydrate, hexamethylenetetramine (HTMA), ethanolamine, methanol, isopropyl alcohol, zinc nitrate hexahydrate, poly-L-lysine (PLL) solution (0.01%), deionized water, Au NP (60 nm diameter, optical density (OD) 1, stabilized suspension in 0.1 mM phosphate-buffered saline, PBS) and Ag NP (60 nm particle size, 0.02 mg/mL in aqueous buffer, containing sodium citrate as stabilizer) were obtained from *Sigma-Aldrich*. ZnO NR were synthesized on a glass substrate using the hydrothermal method following the procedure in the article by Viter et al. [32]. Briefly, after cleaning a glass slide in piranha solution, a ZnO seed layer was prepared by spin casting of 20 μL of 1 mg/mL zinc acetate methanol solution. The sample was annealed at 350°C for 2 h. The glass substrates with ZnO seed layers were incubated for 4 h in 50 mM zinc nitrate and 50 mM of HTMA containing solution in water at 90°C. Thereafter the samples were washed in water and dried at RT.

The colloidal NP were deposited on the surface of ZnO NR in a convective CFA process [3, 30] with a withdrawal velocity 0.1 μm/s. For improved adhesion a set of samples was immersed in a 0.01% PLL solution for 15 min and rinsed with deionized water prior to the deposition of Au and Ag NP. The morphological properties of obtained ZnO-metal assemblies were observed using scanning electron microscopy (SEM, *Hitachi* S4800). Optical properties were measured using an inverted microscope (Olympus IX 71), which was fibre coupled to a UV-VIS-NIR spectrometer (Ocean Optics USB4000) either in the PL mode using a Hg lamp light source (U-LH100HG) with a fluorescence filter set (U-MWU2) or in the micro–extinction spectroscopy (MExS) transmission mode [33] using a halogen lamp (U-LH100-3). Spectra from ZnO samples without any deposited NP were used as reference for MExS measurements. A 10× objective lens (CPLNFLN 10XPH, NA 0.3) was used in all cases.

3. Results and discussion

After hydrothermal growth, the glass slides were covered by a dense layer of ZnO NR with diameters in the 50–100 nm range. Larger (μm size) ZnO crystals were also present (Fig. 1).

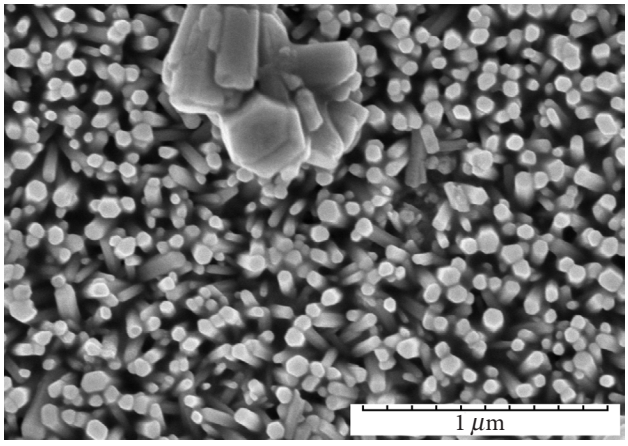

Fig. 1. A SEM image of ZnO NR after immersion in Ag colloid without poly-L-lysine (PLL) surface treatment. Similar images (absent NP) were obtained using Au colloid without PLL treatment and for as synthesized ZnO NR.

For comparison, we first mention the results of ZnO dip-coating without PLL surface treatment. In this case, hardly any NP could be identified in the SEM images of ZnO NR film and the microcrystals (Fig. 1). The absence of NP was also evident by the lack of plasmonic colouring (Fig. 2(b, d)) in diffuse reflection from the macroscopic samples. It can be reasoned that, although wurtzite-type ZnO NP have positive surface charges [34], due to adsorption of negative ions in the citrate and phosphate buffers, the net force on the NP in stabilized colloids may become repulsive. As a result, the NP would be pushed away from the meniscus zone before they can get trapped by capillary forces in the grooves of the nanostructured ZnO surface. Another factor that may hinder the convective CFA colloid assembly is the hydrophobicity of the ZnO NR films [35], which can prevent formation and sustainability of the wetting film and reduce the evaporation surface area. Reduced evaporation flux leads to reduced particle flux towards the three-phase contact line [36]. As a result, the number of NP that deposit on a surface from the relatively dilute colloids was extremely low.

The effect of PLL surface treatment prior to dip-coating becomes obvious as the samples acquire the characteristic plasmonic colouring of Ag (yellow) and Au (pink) NP (Fig. 2(c, e)). For a uniform sample coverage with NP a steady CFA assembly is required, however, on the samples only few mm in size this was limited by the initial meniscus formation and the colloid accumulation at the bottom of the sample. Nevertheless, the uniform regions are of sufficient size for MExS and PL microscopy.

The metal NP after CFA deposition can attach to the ZnO surface deep in the NR film, which makes them difficult to spot in the SEM images. However, a mechanical micro-scratch can reveal the buried NP (Fig. 3) and enable one to estimate the number of particles per unit area to be of the order 10 μm^{-2}. Such concentration of NP is sufficient to cause the distinct LSPR colouring of the samples. For comparison, consider the ruby red original Au

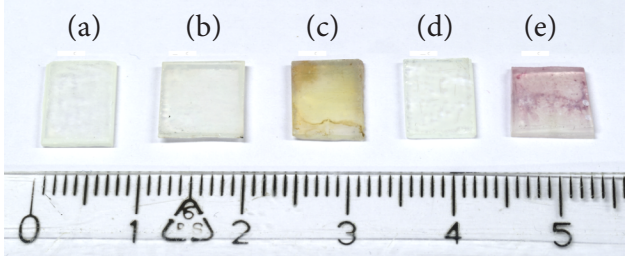

Fig. 2. A photograph of ZnO NR coated samples after different treatments: (a) bare ZnO, (b) dip-coated ZnO-Ag, (c) ZnO-Ag/PLL, (d) ZnO-Au, (e) ZnO-Au/PLL.

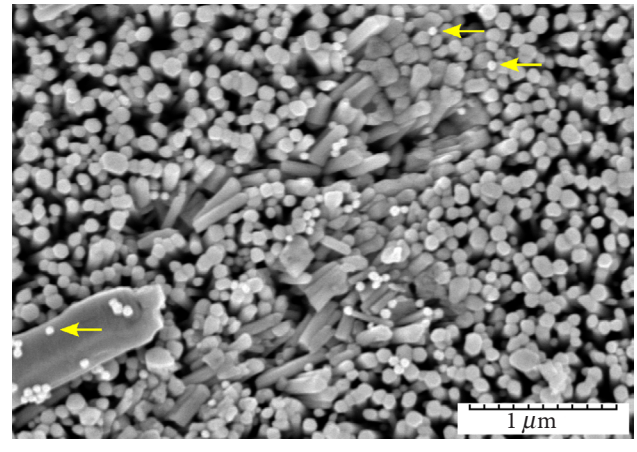

Fig. 3. A SEM image of a micro-scratch area in the ZnO NR film with 60 nm diameter Au NP (few samples marked by arrows) deposited after PLL surface treatment.

colloid (OD 1, with $1.9 \cdot 10^{10}$ particles/mL according to manufacturers' data). If all particles from a 1 cm^3 volume were deposited on a 1 cm^2 surface area, the corresponding coverage density would be 190 μm^{-2}, which is only a single order of magnitude larger than the observed NP density on the ZnO surface with a pink appearance.

A similar NP density can also be found on the facets of the ZnO micro-crystals (Fig. 4). One can observe that the flat micro-crystal surfaces contain larger NP aggregates in comparison to the fine ZnO NR film, which hosts mainly individual NP and small assemblies. This effect is similar to the NP aggregate splitting by NAA films [30]. Finally, we note that for PLL treated samples the number of NP on all ZnO crystal facets is similar without significant preference to crystallographic planes as would be expected for the anisotropic ZnO crystals [22].

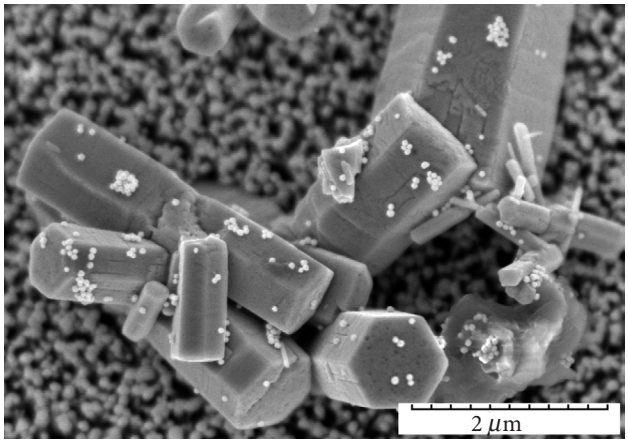

Fig. 4. A SEM image of ZnO microcrystals with Au NP deposited after PLL surface treatment.

The MExS spectra recorded from randomly selected spots on ZnO substrates decorated with Ag and Au NP are shown in Fig. 5. Despite considerable variation, the spectra show a similar wavelength dependence that is clearly different for Ag and Au colloids. According to the manufacturers' data, for the Ag colloid, the extinction peak is expected at 450 nm (in liquid) and 540 nm for Au NP of the same size (60 nm diameter). The extinction peak wavelength for NP on the ZnO surface may differ slightly from that in the buffer solution due to a different effective refractive index of the surrounding medium. Nevertheless, similar peak wavelength values can be presumed in the measured spectra of dry NP on ZnO (Fig. 5). This is

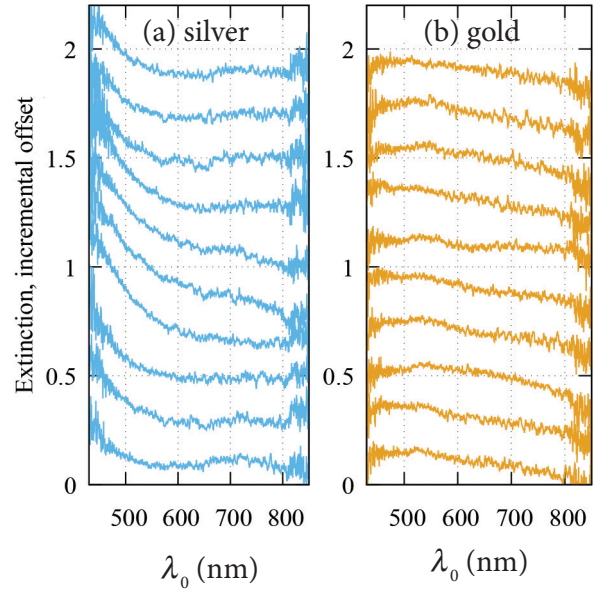

Fig. 5. Micro-extinction spectra ($-\log_{10}(T)$, where T is transmittance) from different spots on (a) ZnO-Ag and (b) ZnO-Au samples. A constant offset is incrementally added to each spectrum for better visibility.

a good indication that a significant number of NPs are isolated and have not aggregated in large clusters. For aggregated Au NP the extinction maximum would shift to a longer wavelength causing a blue/purple appearance of the samples. The difference in spectra can be attributed to the presence of larger ZnO crystals with an uneven distribution across the sample area, which causes different proportions between isolated and aggregated NP.

When illuminated with a UV light from a Hg lamp through the excitation filter 330–385 nm transmission range, the samples emit orange light that can easily be seen by an unaided eye. The PL spectra (Fig. 6(a)) have a maximum at 640 nm or 1.94 eV. The orange emission from hydrothermal ZnO NR has previously been observed [37] and attributed to oxygen interstitials defects on the surface.

The presence of metal NP in our case modified the PL spectra only at shorter wavelengths, below 640 nm. The most notable difference in the PL spectra before and after deposition of NP was found at 560 nm for Au NP on ZnO (Fig. 6(b)). This wavelength corresponds to yellow/green luminescence bands attributed to several defect types in the ZnO structure [9]. This wavelength is also close to the Au NP extinction maximum wavelength (560 nm), which is the likely cause of change of the PL signal. Indeed, the suppression

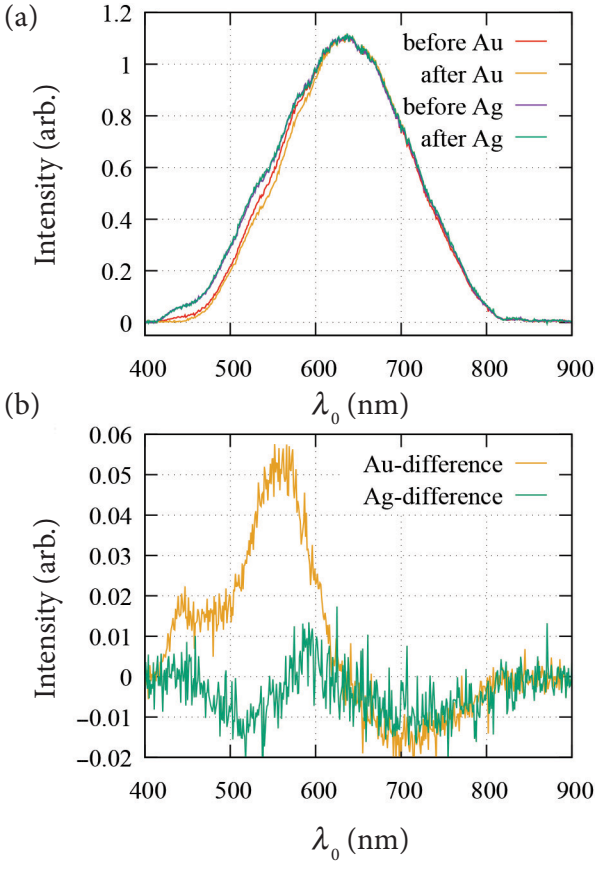

Fig. 6. (a) PL spectra of ZnO with metal NP (after dip-coating) and without metal NP (before dip-coating). (b) Differences of PL spectra before and after dip-coating in colloidal solution.

of defect emission at similar wavelengths in composites of ZnO NR and Au NP has been reported before [38] and explained by the resonant excitation of particle plasmons and a nonradiative decay via the excitation of electron–hole pairs. The explanation also agrees with the absence of similar effects in Ag NP, the LSPR resonance of which does not coincide with the defect emission energy. It should be noted that in our case only few ZnO NR are in contact with metal NP. In spite of that the dip-coating in Au NP colloid caused a notable PL suppression. For comparison, sputtered Au NP with much smaller sizes but a larger contact area with ZnO have been shown to almost completely eliminate the visible PL [39].

4. Conclusions

We have demonstrated a new method of colloidal Au and Ag NP deposition on ZnO NR. The NP density was increased by surface modification using poly-L-lysine solution. Potentially, a higher colloid concentration and repetitive coating could further increase the coverage. Diffuse reflection and MExS show that NP maintain the LSPR characteristic spectra indicating that a significant portion of NP remain isolated (without aggregation) over sufficiently large areas. In comparison to a much weaker effect of Ag NP, the deposition of 60 nm diameter Au colloid caused a significant change in the ZnO nanorod PL intensity with the most pronounced differences at 560 nm emission wavelength. The relationship between PL suppression and LSPR of deposited NP may be useful in development of sensor or photovoltaic devices.

Acknowledgements

The work was performed within the Taiwan-Latvia-Lithuania Cooperation Project LV-LT-TW/2020/5 ‘2D Nanostructures of Noble Metal Nanoparticles for Biosensor Applications’ and the European Union’s Horizon 2020 Research and Innovation Program under Grant Agreement No. 778157 ‘Novel 1D Photonic Metal Oxide Nanostructures for Early Stage Cancer Detection – CanBioSe’. D.K. gratefully acknowledges the Latvian State Scholarship Program.

References

[1] J.W. Kemling, A.J. Qavi, R.C. Bailey, and K.S. Suslick, Nanostructured substrates for optical sensing, J. Phys. Chem. Lett. **2**, 2934 (2011).

[2] R. Viter, Z. Balevicius, A. Abou Chaaya, I. Baleviciute, S. Tumenas, L. Mikoliunaite, A. Ramanavicius, Z. Gertnere, A. Zalesska, V. Vataman, V. Smyntyna, D. Erts, P. Miele, and M. Bechelany, The influence of localized plasmons on the optical properties of Au/ZnO nanostructures, J. Mater. Chem. C **3**, 6815 (2015).

[3] U. Malinovskis, R. Poplausks, D. Erts, K. Ramser, S. Tamulevičius, A. Tamulevičienė, Y. Gu, and J. Prikulis, High-density plasmonic nanoparticle arrays deposited on nanoporous anodic alumina templates for optical sensor applications, Nanomaterials **9**, 531 (2019).

[4] H.H. Mai and E. Janssens, Au nanoparticle–decorated ZnO nanorods as fluorescent non-enzymatic glucose probe, Microchim. Acta **187**, 577 (2020).

[5] A. Tamashevski, Y. Harmaza, E. Slobozhanina, R. Viter, and I. Iatsunskyi, Photoluminescent detection of human T-lymphoblastic cells by ZnO nanorods, Molecules **25**, 3168 (2020).

[6] F. Zhou, W. Jing, S. Liu, Q. Mao, Y. Xu, F. Han, Z. Wei, and Z. Jiang, Electrodeposition of gold nanoparticles on ZnO nanorods for improved performance of enzymatic glucose sensors, Mater. Sci. Semicond. Process. **105**, 104708 (2020).

[7] Z.H. Chen, Y.B. Tang, C.P. Liu, Y.H. Leung, G.D. Yuan, L.M. Chen, Y.Q. Wang, I. Bello, J.A. Zapien, W.J. Zhang, C.S. Lee, and S.T. Lee, Vertically aligned ZnO nanorod arrays sentisized with gold nanoparticles for Schottky barrier photovoltaic cells, J. Phys. Chem. C **113**, 13433 (2009).

[8] T. Bora, D. Zoepfl, and J. Dutta, Importance of plasmonic heating on visible light driven photocatalysis of gold nanoparticle decorated zinc oxide nanorods, Sci. Rep. **6**, 26913 (2016).

[9] Ü. Özgür, Y.I. Alivov, C. Liu, A. Teke, M.A. Reshchikov, S. Doğan, V. Avrutin, S.-J. Cho, and H. Morkoç, A comprehensive review of ZnO materials and devices, J. Appl. Phys. **98**, 041301 (2005).

[10] B.K. Meyer, H. Alves, D.M. Hofmann, W. Kriegseis, D. Forster, F. Bertram, J. Christen, A. Hoffmann, M. Straßburg, M. Dworzak, U. Haboeck, and A.V. Rodina, Bound exciton and donor–acceptor pair recombinations in ZnO, Phys. Status Solidi **241**, 231 (2004).

[11] S. Kuriakose, B. Satpati, and S. Mohapatra, Highly efficient photocatalytic degradation of organic dyes by Cu doped ZnO nanostructures, Phys. Chem. Chem. Phys. **17**, 25172 (2015).

[12] B. Lin, Z. Fu, and Y. Jia, Green luminescent center in undoped zinc oxide films deposited on silicon substrates, Appl. Phys. Lett. **79**, 943 (2001).

[13] Z. Wang, X. Zu, S. Zhu, and L. Wang, Green luminescence originates from surface defects in ZnO nanoparticles, Phys. E Low Dimens. Syst. Nanostruct. **35**, 199 (2006).

[14] T. Serevičius and S. Juršėnas, Growth, properties and sensor applications of low temperature grown ZnO nanorods, Lith. J. Phys. **51**, 309 (2011).

[15] A. Wei, L. Pan, and W. Huang, Recent progress in the ZnO nanostructure-based sensors, Mater. Sci. Eng. B **176**, 1409 (2011).

[16] A.B. Djurišić, Y.H. Leung, K.H. Tam, L. Ding, W.K. Ge, H.Y. Chen, and S. Gwo, Green, yellow, and orange defect emission from ZnO nanostructures: Influence of excitation wavelength, Appl. Phys. Lett. **88**, 103107 (2006).

[17] L. Yang, Q. Zhao, and M. Willander, Size-controlled growth of well-aligned ZnO nanorod arrays with two-step chemical bath deposition method, J. Alloys Compd. **469**, 623 (2009).

[18] S. Baruah and J. Dutta, Hydrothermal growth of ZnO nanostructures, Sci. Technol. Adv. Mater. **10**, 013001 (2009).

[19] J. Li, X. Chen, H. Li, M. He, and Z. Qiao, Fabrication of zinc oxide nanorods, J. Cryst. Growth **233**, 5 (2001).

[20] A. Abou Chaaya, R. Viter, M. Bechelany, Z. Alute, D. Erts, A. Zalesskaya, K. Kovalevskis, V. Rouessac, V. Smyntyna, and P. Miele, Evolution of microstructure and related optical properties of ZnO grown by atomic layer deposition, Beilstein J. Nanotechnol. **4**, 690 (2013).

[21] A. Kołodziejczak-Radzimska and T. Jesionowski, Zinc oxide – from synthesis to application: A review, Materials (Basel) **7**, 2833 (2014).

[22] C.G. Read, E.M.P. Steinmiller, and K.-S. Choi, Atomic plane-selective deposition of gold nanoparticles on metal oxide crystals exploiting preferential adsorption of additives, J. Am. Chem. Soc. **131**, 12040 (2009).

[23] K.A. Willets and R.P. Van Duyne, Localized surface plasmon resonance spectroscopy and sensing, Annu. Rev. Phys. Chem. **58**, 267 (2007).

[24] K. Nakaji, H. Li, T. Kiba, M. Igarashi, S. Samukawa, and A. Murayama, Plasmonic enhancements of photoluminescence in hybrid Si nanostructures with Au fabricated by fully top-down lithography, Nanoscale Res. Lett. **7**, 629 (2012).

[25] U. Malinovskis, R. Poplausks, I. Apsite, R. Meija, J. Prikulis, F. Lombardi, and D. Erts, Ultrathin anodic aluminum oxide membranes for production of dense sub-20 nm nanoparticle arrays, J. Phys. Chem. C **118**, 8685 (2014).

[26] J. Prikulis, U. Malinovskis, R. Poplausks, I. Apsite, G. Bergs, and D. Erts, Optical scattering by dense disordered metal nanoparticle arrays, Plasmonics **9**, 427 (2014).

[27] Q. Zhang, J. Xie, Y. Yu, and J.Y. Lee, Monodispersity control in the synthesis of monometallic and bimetallic quasi-spherical gold and silver nanoparticles, Nanoscale **2**, 1962 (2010).

[28] U.K. Makhmanov, A. Kokhkharov, S. Bakhramov, and D. Erts, The formation of self-assembled structures of C_{60} in solution and in the volume of an evaporating drop of a colloidal solution, Lith. J. Phys. **60** (2020).

[29] J.M. Romo-Herrera, R.A. Alvarez-Puebla, and L.M. Liz-Marzán, Controlled assembly of plasmonic colloidal nanoparticle clusters, Nanoscale **3**, 1304 (2011).

[30] U. Malinovskis, A. Berzins, F. Gahbauer, R. Ferber, G. Kitenbergs, I. Muiznieks, D. Erts, and J. Prikulis, Colloidal nanoparticle sorting and ordering on anodic alumina patterned surfaces using templated capillary force assembly, Surf. Coatings Technol. **326**, 264 (2017).

[31] F. Ghilini, M.C. Rodríguez González, A.G. Miñán, D. Pissinis, A.H. Creus, R.C. Salvarezza, and P.L. Schilardi, Highly stabilized nanoparticles on poly-L-lysine-coated oxidized metals: a versatile platform with enhanced antimicrobial activity, ACS Appl. Mater. Interfaces **10**, 23657 (2018).

[32] R. Viter, K. Kunene, P. Genys, D. Jevdokimovs, D. Erts, A. Sutka, K. Bisetty, A. Viksna, A. Ramanaviciene, and A. Ramanavicius, Photoelectrochemical bisphenol S sensor based on ZnO-nanoroads modified by molecularly imprinted polypyrrole, Macromol. Chem. Phys. **221**(2), 1900232 (2019).

[33] A. Kumar, E. Villarreal, X. Zhang, and E. Ringe, Micro-extinction spectroscopy (MExS): a versatile optical characterization technique, Adv. Struct. Chem. Imaging **4**, 8 (2018).

[34] K.-M. Kim, M.-H. Choi, J.-K. Lee, Y.-R. Jeong, J. Kim, M.-K. Kim, S.-M. Paek, and J.-M. Oh, Physicochemical properties of surface charge-modified ZnO nanoparticles with different particle sizes, Int. J. Nanomedicine **9**, 41 (2014).

[35] X. Feng, L. Feng, M. Jin, J. Zhai, L. Jiang, and D. Zhu, Reversible super-hydrophobicity to super-hydrophilicity transition of aligned ZnO nanorod films, J. Am. Chem. Soc. **126**, 62 (2004).

[36] A.S. Dimitrov and K. Nagayama, Continuous convective assembling of fine particles into two-dimensional arrays on solid surfaces, Langmuir **12**, 1303 (1996).

[37] L. Wu, Y. Wu, X. Pan, and F. Kong, Synthesis of ZnO nanorod and the annealing effect on its photoluminescence property, Opt. Mater. (Amst) **28**, 418 (2006).

[38] H.Y. Lin, C.L. Cheng, Y.Y. Chou, L.L. Huang, Y.F. Chen, and K.T. Tsen, Enhancement of band gap emission stimulated by defect loss, Opt. Express **14**, 2372 (2006).

[39] M. Liu, R. Chen, G. Adamo, K.F. MacDonald, E.J. Sie, T.C. Sum, N.I. Zheludev, H. Sun, and H.J. Fan, Tuning the influence of metal nanoparticles on ZnO photoluminescence by atomic-layer-deposited dielectric spacer, Nanophotonics **2**, 153 (2013).

KOLOIDINIŲ METALO NANODALELIŲ NUSODINIMAS ANT CINKO OKSIDO NANOSTRYPELIŲ IR JŲ ĮTAKA REGIMAJAI FOTOLIUMINESCENCIJAI

D. Kulmatova [a, b], M. Baitimirova [a], U. Malinovskis [a], C.-F. Chang [c], Y. Gu [d], A. Tamulevičienė [e], D. Erts [a, f], J. Prikulis [a]

[a] *Latvijos universiteto Cheminės fizikos institutas, Ryga, Latvija*

[b] *Uzbekistano nacionalinis universitetas, Taškentas, Uzbekistanas*

[c] *Tunghai universiteto Aplinkos mokslo ir inžinerijos fakultetas, Taichungas, Taivanas*

[d] *Tunghai universiteto Chemijos ir medžiagų inžinerijos fakultetas, Taichungas, Taivanas*

[e] *Kauno technologijos universiteto Medžiagų mokslo institutas, Kaunas, Lietuva*

[f] *Latvijos universiteto Chemijos fakultetas, Ryga, Latvija*

Santrauka

Analizuota koloidinių aukso (Au) ir sidabro (Ag) nanodalelių įtaka hidrotermiškai užaugintų ZnO nanostrypelių optinėms savybėms. Individualios 60 nm skersmens nanodalelės ir jų mažos sankaupos išvengiant didelių agregatų buvo nusodintos ant poli-L-lizinu padengtų nanostrypelių nardinimo būdu. Suformuotų ZnO-metalo hibridų morfologija ir optinės savybės buvo įvertintos naudojantis atitinkamai skenuojančiu elektronų mikroskopu bei fotoliuminescencijos ir difuzinio atspindžio spektroskopijomis. Nustatyta, kad Au nanodalelės selektyviai slopina ZnO nanostrypelių fotoliuminescencijos signalą ties 560 nm, kuris susijęs su ZnO paviršiniais defektais. Tuo tarpu vienodo dydžio Ag nanodalelės turėjo tik nežymią įtaką fotoliuminescencijos signalui. Pristatomi rezultatai gali būti naudingi valdant hibridinių medžiagų optines savybes tobulinant jutiklius ar fotovoltinius prietaisus.